PREDICTION OF THREE DIMENSIONAL NATURAL CONVECTION FROM A HORIZONTAL ISOTHERMAL SQUARE PLATE

Ayad K. Hassan
University of Technology/Material Dept.

ABSTRACT

A theoretical study of a three-dimensional natural convection heat transfer from an isothermal horizontal square plate, with upper and lower heated surfaces is present. The transient Navier–Stokes and energy equations were solved by using finite deference method (F.D.M). The complete Navier–Stokes equations are transformed and expressed in terms of vorticity–vector potential and solved using an Alternating Direction Implicit (ADI) method for the parabolic portion of the problem, and Successive Over–Relaxation (SOR) method for the elliptic portion .A computer program in (FORTRAN 77) was built to carry out the solution. The numerical results were obtained for laminar flow range of Grashof number up to (10^5) in up ward–facing and downward–facing with Prandtl number of (0.72). The results of local Nusselt number have maximum values at the outer edge of plate for two cases upward and downward facing heating. The comparison of the results of average Nusselt number with numerical data for downward facing and experimental data for upward facing shows acceptable agreement. It may be noted that the present data are generally different with experimental data, since the available data are extrapolated to high Grashof number. Thus the deviation may be large with present data.

الخلاصه

يقدم هذا البحث دراسة نظرية لانتقال الحرارة ثلاثي الابعاد للحمل الطبيعي من صفيحةمربعةبوضع افقي تكون مسخنة من الاعلى والاسفل .تتضمن الدراسة الحل العددي لمعادلة الزخم والطاقة الانتقالية باستخدام طريقة الفروق المحددة .معادلة الزخم الكاملة تم تحويلها والتعبير عنها بدلالة الدوامية _متجه دالة الانسياب . المعادلات المحولة تم حلها باستخدام طريقة الاتجاه الضمني للجزء القطعي مكافئ من المسالة وطريقة فوق التراخي للجزء البيضوي .تم بناء برنامج بلغة فورتران 77لتنفيذ الحل العددي ,الذي يغطي الصحيفة مسخنة للاسفل مربعة الشكلة افقية .النتائج العددية التي تم الحصول عليهاضمن الجريان الطبقي الى حد رقم كراشوف 10^5مع رقم برانتل(0.75).رقم نسلت الموضعي تكون اعلى قيمة له عند الحافة للصفيحة للحالتين الوجه المسخن للاعلى والاسفل.تم مقارنة النتائج الحالية لرقم نسلت المعدل مع نتائج عددية وكذلك لحالة الصفيحة الوجه المسخن للاسفل وكان هناك توافق بين النتائج .وكذلك مقارنة النتائج للبحث الحالي للحالة الصفيحة الوجه المسخن الى الاعلى مع نتائج عددية وعملية نلاحظ هناك توافق في النتائج العددية وهناك فارق في النتائج العملية.

KEYWORD : Natural Convection , Three Dimensional, Isothermal ,Square Plate

INTRODUCTION

In resent years, natural convection heat Transfer from finite size bodies such as (square surface) has attracted much attention with relation to the electronic cooling industry. The problem of natural convection heat Transfer from square plate continues to be a topic of current research, and also a number of theoretical and experimental studies **(Boehm and Kamyab 1968), (Aihara et. al.1971), (Aziz and Hellums 1967) and (Rafa 2002)** have been made in the past to determine the natural convection heat Transfer from a heated plate held in the horizontal position, one of the earliest studies **(Rafa 2002)** has been done experimentally for horizontal and inclined positions

for a square plate under conditions of constant temperature, and studied theoretically the two dimensional problem of upward–facing. The problem of natural convection from horizontal facing upward and downward with constant temperature wall conditions has been the subject of considerable interest and controversy. Since the natural convection flow above and below the heated square plate is three dimensional flow, the purpose of the work presented here is to develop a numerical calculations algorithm suitable for solution of the three–dimensional problem of laminar natural convection heat transfer from square plate upward and downward facing with constant wall temperature. Three dimensional time dependent governing equations in term of a vorticity–vector potential form and Temperature are solved numerically, using for the temperature and vorticity vector the Alternating Direction Implicit (ADI) method since this method is stable for three dimensions, and for vector potential a point iterative Successive over relaxation (SOR) method is used. The main theoretical investigations were made to investigate the effect of edges of a square plate on local natural convection heat transfer coefficient and to study the effect of position (up or down face) on the Nusselt Number.

MATHEMATICAL MODEL

In natural convection, a consideration of fluid flow is necessary in the study of energy and mass transfer mechanisms. A study of convection further necessitates consideration of the coupling between the fluid flow and the mechanisms underlying conduction. This is due to the fact that heat transported due to a moving fluid element would eventually be transformed to its´ neighboring elements through conduction. Moreover, in regions close to surface, which is at a temperature different from that of the ambient medium, there is no relative motion between the surface and the fluid, and the transfer of energy is predominated by conduction.

Natural convection above and below the square plate of **Fig.**1 is described by the equations for the conservation of mass, momentum and energy in x , y and z directions simplified in accordance with Boussinesq assumption. The components of gravity in the x, y and z directions for facing upward are 0, 0, – g respectively. Taking a cross derivatives of momentum equations and subtracting out the pressure terms, introducing the vorticity and nondimensionalizing then yields the following dimensionless vorticity and energy equations, **(Aziz and Hellums 1967);**

$$\frac{1}{\mathrm{Pr}}\frac{\partial \Omega_1}{\partial \tau}+\mathrm{U}\frac{\partial \Omega_1}{\partial \mathrm{X}}+\mathrm{V}\frac{\partial \Omega_1}{\partial \mathrm{Y}}+\mathrm{W}\frac{\partial \Omega_1}{\partial \mathrm{Z}}-\Omega_1\frac{\partial \mathrm{U}}{\partial \mathrm{X}}-\Omega_2\frac{\partial \mathrm{V}}{\partial \mathrm{Y}}-\Omega_3\frac{\partial \mathrm{W}}{\partial \mathrm{Z}}=\frac{\partial^2 \Omega_1}{\partial \mathrm{X}^2}+\frac{\partial^2 \Omega_1}{\partial \mathrm{Y}^2}+\frac{\partial^2 \Omega_1}{\partial \mathrm{Z}^2}+\mathrm{Ra}\frac{\partial \mathrm{T}}{\partial \mathrm{Y}} \qquad (1)$$

$$\frac{1}{\mathrm{Pr}}\frac{\partial \Omega_2}{\partial \tau}+\mathrm{U}\frac{\partial \Omega_2}{\partial \mathrm{X}}+\mathrm{V}\frac{\partial \Omega_2}{\partial \mathrm{Y}}+\mathrm{W}\frac{\partial \Omega_2}{\partial \mathrm{Z}}-\Omega_1\frac{\partial \mathrm{U}}{\partial \mathrm{X}}-\Omega_2\frac{\partial \mathrm{V}}{\partial \mathrm{Y}}-\Omega_3\frac{\partial \mathrm{W}}{\partial \mathrm{Z}}=\frac{\partial^2 \Omega_2}{\partial \mathrm{X}^2}+\frac{\partial^2 \Omega_2}{\partial \mathrm{Y}^2}+\frac{\partial^2 \Omega_2}{\partial \mathrm{Z}^2}+\mathrm{Ra}\frac{\partial \mathrm{T}}{\partial \mathrm{X}} \qquad (2)$$

$$\frac{1}{\mathrm{Pr}}\frac{\partial \Omega_3}{\partial \tau}+\mathrm{U}\frac{\partial \Omega_3}{\partial \mathrm{X}}+\mathrm{V}\frac{\partial \Omega_3}{\partial \mathrm{Y}}+\mathrm{W}\frac{\partial \Omega_3}{\partial \mathrm{Z}}-\Omega_1\frac{\partial \mathrm{U}}{\partial \mathrm{X}}-\Omega_2\frac{\partial \mathrm{V}}{\partial \mathrm{Y}}-\Omega_3\frac{\partial \mathrm{W}}{\partial \mathrm{Z}}=\frac{\partial^2 \Omega_3}{\partial \mathrm{X}^2}+\frac{\partial^2 \Omega_3}{\partial \mathrm{Y}^2}+\frac{\partial^2 \Omega_3}{\partial \mathrm{Z}^2}0 \qquad (3)$$

$$\frac{\partial \mathrm{T}}{\partial \tau}+\mathrm{U}\frac{\partial \mathrm{T}}{\partial \mathrm{X}}+\mathrm{V}\frac{\partial \mathrm{T}}{\partial \mathrm{Y}}+\mathrm{W}\frac{\partial \mathrm{T}}{\partial \mathrm{Z}}=\frac{\partial^2 \mathrm{T}}{\partial \mathrm{X}^2}+\frac{\partial^2 \mathrm{T}}{\partial \mathrm{Y}^2}+\frac{\partial^2 \mathrm{T}}{\partial \mathrm{Z}^2} \qquad (4)$$

The components of dimensionless vorticity are **(Aziz and Hellums 1967).**

$$\Omega_1=\frac{\partial \mathrm{W}}{\partial \mathrm{Y}}-\frac{\partial \mathrm{V}}{\partial \mathrm{Z}} \qquad (5)$$

$$\Omega_2=\frac{\partial \mathrm{U}}{\partial \mathrm{Z}}-\frac{\partial \mathrm{W}}{\partial \mathrm{X}} \qquad (6)$$

$$\Omega_3=\frac{\partial \mathrm{V}}{\partial \mathrm{X}}-\frac{\partial \mathrm{U}}{\partial \mathrm{Y}} \qquad (7)$$

To calculate the velocity from vorticity ,it is convenient to introduce a vector potential $\vec{\Psi}$,which may be looked upon as the three dimensional counterpart of two dimension stream function. The component of the velocity are related to the components of dimensionless vector potential, the dimensionless vector potential is defined such that its curl equals the dimensionless velocity vector **(Aziz and Hellums 1967);**

$$\vec{V} = \nabla \times \vec{\Psi} \tag{8}$$

$$U = \frac{\partial \Psi_3}{\partial Y} - \frac{\partial \Psi_2}{\partial Z} \tag{9}$$

$$V = \frac{\partial \Psi_1}{\partial Z} - \frac{\partial \Psi_3}{\partial X} \tag{10}$$

$$W = \frac{\partial \Psi_2}{\partial X} - \frac{\partial \Psi_1}{\partial Y} \tag{11}$$

The vector potential satisfies the continuity equation

$$\nabla.\vec{V} = \nabla.(\nabla \times \vec{\Psi}) \tag{12}$$

This vector potential is assumed to be solenoidal, i.e.

$$\frac{\partial \Psi_1}{\partial X} + \frac{\partial \Psi_2}{\partial Y} + \frac{\partial \Psi_3}{\partial Z} = 0 \tag{13}$$

The components of the dimensionless velocity are related to the component of the dimensionless vector potential as follows;

$$-\Omega_1 = \frac{\partial^2 \Psi_1}{\partial X^2} + \frac{\partial^2 \Psi_1}{\partial Y^2} + \frac{\partial^2 \Psi_1}{\partial Z^2} \tag{14}$$

$$-\Omega_2 = \frac{\partial^2 \Psi_2}{\partial X^2} + \frac{\partial^2 \Psi_2}{\partial Y^2} + \frac{\partial^2 \Psi_2}{\partial Z^2} \tag{15}$$

$$-\Omega_3 = \frac{\partial^2 \Psi_3}{\partial X^2} + \frac{\partial^2 \Psi_3}{\partial Y^2} + \frac{\partial^2 \Psi_3}{\partial Z^2} \tag{16}$$

BOUNDARY AND INITIAL CONDITIONS.

At $\tau = 0$

$\Psi_1 = \Psi_2 = \Psi_3 = \Omega_1 = \Omega_2 = \Omega_3 = U = V = W = 0$ At any point in the domain

$T = 1$ at the heated surface

At $\tau > 0$

At $Z = 0$ $\quad 0 \le X \le 1$ and $0 \le Y \le 0.5$ $\quad T = 1$

At $Z = 2$ $\quad 0 \le X \le 1$ and $0 \le Y \le 0.5$ $\quad T = 0$

At $X = 0$ and $X = 1$ $\quad 0 \le Z \le 2$ and $0 \le Y \le 0.5$ $\quad T = 0$

At $Y = 0$ and $Y = 0.5$ $\quad 0 \le Z \le 2$ and $0 \le X \le 1$ $\quad T = 0$

Vector potential

At $Z = 0$ $\quad 0 \le X \le 1$ and $0 \le Y \le 0.5$

$$\Psi_1 = \Psi_2 = \frac{\partial \Psi_3}{\partial Z} = 0$$

At $Z = 2$ $0 \le X \le 1$ and $0 \le Y \le 0.5$

$\Psi_1 = \Psi_2 = \Psi_3 = 0$

At $X = 0$ and $X = 1$ $0 \le Z \le 2$ and $0 \le Y \le 0.5$

$\Psi_1 = \Psi_2 = \Psi_3 = 0$

At $Y = 0$ and $Y = 0.5$ $0 \le Z \le 2$ and $0 \le X \le 1$

$\Psi_1 = \Psi_2 = \Psi_3 = 0$

Vorticity Vector

At $Z = 0$ $0 \le X \le 1$ and $0 \le Y \le 0.5$

$\Omega_1 = -\frac{\partial V}{\partial Z}$, $\Omega_2 = \frac{\partial U}{\partial Z}$, $\Omega_3 = 0$

At $Z = 2$ $0 \le X \le 1$ and $0 \le Y \le 0.5$

$\Omega_1 = \Omega_2 = \Omega_3 = 0$

At $X = 0$ and $X = 1$ $0 \le Z \le 2$ and $0 \le Y \le 0.5$

$\Omega_1 = \Omega_2 = \Omega_3 = 0$

At $Y = 0$ and $Y = 0.5$ $0 \le Z \le 2$ and $0 \le X \le 1$

$\Omega_1 = \Omega_2 = \Omega_3 = 0$

NUMERICAL FORMULATION

In finite difference approximation of partial differential equations the solution of the three components of vorticity and energy **Eqs.** (1), (2), (3) and (4) may be obtained by writing them as follows;

$$\frac{\partial T}{\partial \tau} = \frac{\partial^2 T}{\partial X^2} - U\frac{\partial T}{\partial X} + \frac{\partial^2 T}{\partial Y^2} - V\frac{\partial T}{\partial Y} + \frac{\partial^2 T}{\partial Z^2} - W\frac{\partial T}{\partial Z} \quad (17)$$

$$\frac{\partial \Omega_1}{\partial \tau} = \Pr\frac{\partial^2 \Omega_1}{\partial X^2} - U\frac{\partial \Omega_1}{\partial X} + \Pr\frac{\partial^2 \Omega_1}{\partial Y^2} - V\frac{\partial \Omega_1}{\partial Y} + \Pr\frac{\partial^2 \Omega_1}{\partial Z^2} - W\frac{\partial \Omega_1}{\partial Z} + S_1 \quad (18)$$

$$\frac{\partial \Omega_2}{\partial \tau} = \Pr\frac{\partial^2 \Omega_2}{\partial X^2} - U\frac{\partial \Omega_2}{\partial X} + \Pr\frac{\partial^2 \Omega_2}{\partial Y^2} - V\frac{\partial \Omega_2}{\partial Y} + \Pr\frac{\partial^2 \Omega_2}{\partial Z^2} - W\frac{\partial \Omega_2}{\partial Z} + S_2 \quad (19)$$

$$\frac{\partial \Omega_3}{\partial \tau} = \Pr\frac{\partial^2 \Omega_3}{\partial X^2} - U\frac{\partial \Omega_3}{\partial X} + \Pr\frac{\partial^2 \Omega_3}{\partial Y^2} - V\frac{\partial \Omega_3}{\partial Y} + \Pr\frac{\partial^2 \Omega_3}{\partial Z^2} - W\frac{\partial \Omega_3}{\partial Z} + S_3 \quad (20)$$

Where;

$S_1 = \mathrm{Ra}\frac{\partial T}{\partial Y}$

$S_2 = \mathrm{Ra}\frac{\partial T}{\partial X}$

$S_3 = 0$

General form;

$$\frac{\partial \chi}{\partial \tau} = (\delta_X + \delta_Y + \delta_Z)\chi + S \quad (21)$$

Using the Alternating Direction Implicit (ADI) method, the solution of **Eq.** (21)is;

$$(\delta_X - \frac{2}{\Delta\tau})\chi^{*}_{n+1} = -(\delta_X + 2\delta_Y + 2\delta_Z + \frac{2}{\Delta\tau})\chi_n - 2S \quad (21a)$$

$$(\delta_Y - \frac{2}{\Delta\tau})\chi^{**}_{n+1} = \delta_Y\chi_n - \frac{2}{\Delta\tau}\chi^{*}_{n+1} \quad (21b)$$

$$(\delta_Z - \frac{2}{\Delta\tau})\chi_{n+1} = \delta_Z\chi_n - \frac{2}{\Delta\tau}\chi^{**}_{n+1} \quad (21c)$$

The application of the above algorithm to χ_n involves the solution of try diagonal system of linear algebraic equations, three times to obtain χ_{n+1}.

The three equations of vector potential components Ψ_1, Ψ_2 and Ψ_3 can be solved for any time-step by using a point iterative successive over relaxation method.

$$\Psi_{(i,j,k)} = \frac{1}{b}(\Psi_{(i-1,j,k)} + \Psi_{(i+1,j,k)} + \Psi_{(i,j-1,k)} + \Psi_{(i,j+,k)} + \Psi_{(i,j,k-1)} + \Psi_{(i,j,k+1)} + S) \quad (22)$$

A relaxation factor W_Ψ was defined as follows,

$$\Psi^{n(s+1)}_{(i,j,k)} = \Psi^{n}_{(i,j,k)} + W_\Psi(\Psi^{n}_{(i,j,k)} - \Psi^{n(s)}_{(i,j,k)}) \quad (23)$$

Where the counter (s) refers to the number of successive point iterations performed at the n^{th} time step, and $\Psi^{n(s+1)}_{(i,j,k)}$ is the value of the component Ψ at the n^{th} time step after (s+1) iterations. the values of $\Psi^{n(s+1)}_{(i,j,k)}$ are resubstituted into **Eq.**22 which is then solved with **Eq.**23 until the following convergence criterion is satisfied

$$\sum(\Psi^{n(s+1)}_{(i,j,k)} - \Psi^{n(s)}_{(i,j,k)}) \le \varepsilon$$

Where $\varepsilon = 10^{-3}$. The relaxation factor W_Ψ was in the range (1-2) the optimum value of 1.7 was obtained by trial and error.

The local Nusselt number defined as,

$$Nu = \frac{hH}{K} \longrightarrow Nu = -\frac{\partial T}{\partial Z}_{Z=0} \quad (24)$$

which can be solve by forward finite difference for four point . The average Nusselt number is defined as $\overline{Nu} = \frac{1}{A}\iint_A NudA$. This integration can be carried out by the trapezoidal rule **(Torrance 1985).**

The above equations were approximated by finite difference equations and solved by the general three dimensional ADI (alternating direction implicit) method developed by **(Aziz and Hellums 1967).**

The steady–state was computed transiently starting from the static. The energy equation (4) was first solved for a time step, then the three vorticity equations. The vector potential at each grid point was next computed from the known vorticity by using three dimensional (S.O.R) successive over–relaxation methods.

The computations were carried out for only one half of the computational domain since symmetry in terms of the central vertical plane was expected.

RESULTS AND DISCUSSION

Fig.2 shows the isothermal line at section y = 1/2 for different Grashof number ($Gr = 10^3$, $Gr = 10^4$ and $Gr = 10^5$) respectively at late – time steady – state condition. It is clear from the figure that the temperature gradient above the surface of the heated plate increased rapidly in the vicinity of the free edge. In the case of upward facing, the boundary layers from all sides of the heated plate were observed to join and rise as a plume, without any flow reversal. Temperature profiles in the case of facing downward are more stable than those of facing upward case. The effect of convection for Grashof number of (10^4) is clear by the appearance of the plume over the heated surface.

Fig.3 shows the y – component of vector potential Ψ_2 at section y = 1/2 for different Grashof number (10^3, 10^4 and 10^5),respectively, and for two cases upward and downward facing at late–time steady state condition. In the case of upward facing the center of cells move to the outer portion of domain because of the increase in velocity at the center due to the increase in temperature that causes an increase in buoyancy force at the center, and fluid moves down due to the increase in weight. In case of downward facing most of fluid flows toward the center portion of the plate horizontally enters into the boundary layer and flows toward edge in the boundary layer.

Fig.4 shows the contour line of Y-component of vorticity Ω_2 at section Y = ½ in X-Z plane for Grashof numbers (10^3 , 10^4 , 10^5) respectively, for upward and downward facing at late time for steady state condition. In both cases of upward and downward facing, the distribution is symmetric, but the values of contour lines for downward facing are less than the values of contour lines for upward facing for the small effect of convection in downward facing, and to the direction of vorticity opposite that of facing upward. It is clear from **Fig.4** that the values of contour lines increase with the increase of Grashof number.

Fig.5 shows the velocity vector in X-Z plane at section Y = ½ for Grashof numbers (10^3 , 10^4 , 10^5) respectively, for upward and downward facing cases at late time for steady state condition. In both cases the distribution is symmetric. We notice that for high Grashof number more violent because of convection effect. For the case of upward facing, particular attention is paid to the region near the heated surface. The fluid is drawn from all sides and below and increases its velocity near the center. The velocity at the center line, velocity in the flow within a very short distance. This is obviously due to the continuing effect of buoyancy force, which is maximum at the centerline due to the temperature being highest there, because the buoyancy force is directed outward normal to its heated surface. The fluid is pulled from the edge then moves away from the heated surface owing to the outward buoyancy. For the case of downward facing, the buoyancy force is directed inwards normal to its active surface, the fluid is drawn inward towards the center and moves outward towards the edges. The distribution of local Nusselt number for the two cases for Grashof number of (10^3 , 10^4 , 10^5) respectively, is shown in **Fig.7**.

Referring to **Fig.6**, the local Nusselt number have very small changes for the two cases because of the very small effect of convection mode of heat transfer exists, since at low Grashof number the mode of heat transfer is conduction only. The local Nusselt number has maximum values at the outer edge of the plate. The values of local Nusselt in the case of downward facing is less than the values of upward facing.

Fig.7 and **Fig.8** show the local Nusselt along X at Y = ½, the maximum value at the outer edge and minimum value at the center of the plate for the two cases. In general with thickening of boundary layer as flow proceeds downstream from the leading edge, the local Nusselt number gradually decreases. Due to realignment of the flow, velocity levels increase sharply and this is reflected in an increase in the local Nusselt number.

Fig.9 and **Fig.10** show the average Nusselt number with time. **Fig.11** presents the general correlation of the average Nusselt number for the two cases for the plate. The general equation of the average Nusselt number facing upward and downward for plate is in the form: $\overline{Nu} = cRa^n$

Fig.11 shows a comparison of the average Nusselt number $\overline{Nu}$ with numerical results of **(Goldstin et.al. 1983)** and experimental results of of **(Goldstin et.al. 1983)** and **(Rafah 2002)** for facing upward .it may be noted that the present data are generally different with his experimental data ,since the available data are extrapolated to Grashof number thus the deviation may be large. **Fig.12** shows a comparison of present data of average Nusselt number $\overline{Nu}$ with numerical and experimental results of of **(Goldstin et.al. 1983)** for horizontal square plat facing downward

CONCLUSIONS

The numerical results of natural convection heat transfer from horizontal square plate with constant wall temperature, upward and downward facing, has been obtained in the present work. The numerical results were obtained for laminar flow range of Grashof number up to (10^5) in upward and downward–facing with Prandtl number of (0.72). The local Nusselt number have maximum values at the outer edge of plate for the two cases . The comparison of the results of average Nusselt number with numerical data for downward facing and experimental data for upward facing shows acceptable agreement. It is concluded that the present data are generally different with experimental data, since the available data are extrapolated to high Grashof number. Thus the deviation may be large with present data.

REFERENCES

Aihara T., Ozo,H. and Tein,C.L. (1971) "Free Convection Along The Downward-Facing Surface of A Heated Horizontal Plate". Int. J. Heat Mass Transfer. Vol.15, pp. 2535-2549.

Ayad K. Hassan (2003) "Prediction of Three Dimensional Natural Convection from Heated Disk and Rings at Constant Temperature". Eng.&Technology,5,22,

Aziz K. and. Hellums J.D (1967) "Numerical Solution of The Three Dimensional Equations of Motion for Laminar Natural Convection". The Physics of Fluids. 10, 2, 314-325.

Boehm R.F. and Kamyab D. (1977) "Established Strip-wise Laminar Natural Convection on A Horizontal Surface". Transactions of the ASME. Vol. 99, pp. 294-299,

Goldstein R.J.,Kei-Shun Law and Takata,Y. (1983) "Laminar Natural Convection From A Horizontal Plate and The Influence of Plate-edge Extensions". J. Fluid mech. Vol.120, pp. 55-75.

Hatfield D.W. and Edwards D.K. (1981)"Edge and Aspect Ratio Effects on Natural Convection From the Horizontal Heated Plate Facing Downwards". Int.J. Heat Mass Transfer. Vol.24, No.6, pp. 1019-1024.

Husar R.B. and. Sparrow E.M (1968) "Patterns of Free Convection Flow Adjacent to Horizontal Heated Surfaces" Int.J. Heat Mass Transfer. Vol.11, pp. 1206-1208,

Jaluria Y. (1980), "Natural Convection Heat Transfer", Pergamon press.

Rafa Aziz (2002) "Instruction System to Study Free Convection Heat Transfer from Isothermal Square Flat Surface" .M.Sc Thesis Univ. Technology .

Torrance K.E. (1985), "Numerical Method in Heat Transfer", Handbook of Heat Transfer Fundamentals, McGraw-Hill, 2nd Edition.

NOMENCLATURES

H: side length of square plate
h: heat transfer coefficient[$w/m^2.^\circ k$]

k: thermal conductivity[w/m . k]
X: dimensionless X-coordinate =x/H
Y: dimensionless Y-coordinate =y/H
Z: dimensionless Z-coordinate =z/H
T: dimensionless temperature = $\frac{\Theta - \Theta_\infty}{\Theta_w - \Theta_\infty}$
U: dimensionless X-component of velocity =uH/α
u: X-component of velocity[m / s]
V: dimensionless Y-component of velocity =vH/α
v: Y-component of velocity[m/s]
W: dimensionless Z-component of velocity =wH/α
w: Z-component of velocity[m/s]
$\vec{g}$: gravitational vector[m/s^2]

Greek Symbols

α: thermal diffusivity of air[m^2/s]
β: volumetric coefficient of expansion with temperature[1/K]
υ: kinematics viscosity of air[m^2/s]
τ: dimensionless time = tα/H^2

$\vec{\Psi}$: dimensionless vector potential
$\vec{\Omega}$: dimensionless vorticity vector
Θ: temperature [K]

Subscripts

∞ : ambient
w : value of surface
1: vector component in X-direction

3: vector component in Z-direction

DIMENSIONLESS NUMBERS

R_a: Rayleigh number = $\frac{g\beta(\Theta_w - \Theta_\infty)H^3}{\upsilon\alpha}$

G_r: Grashof number = $\frac{g\beta(\Theta_w - \Theta_\infty)H^3}{\upsilon^2}$

Nu: local Nusselt number = $\frac{hH}{K}$

Pr: Prandtl number = υ/α

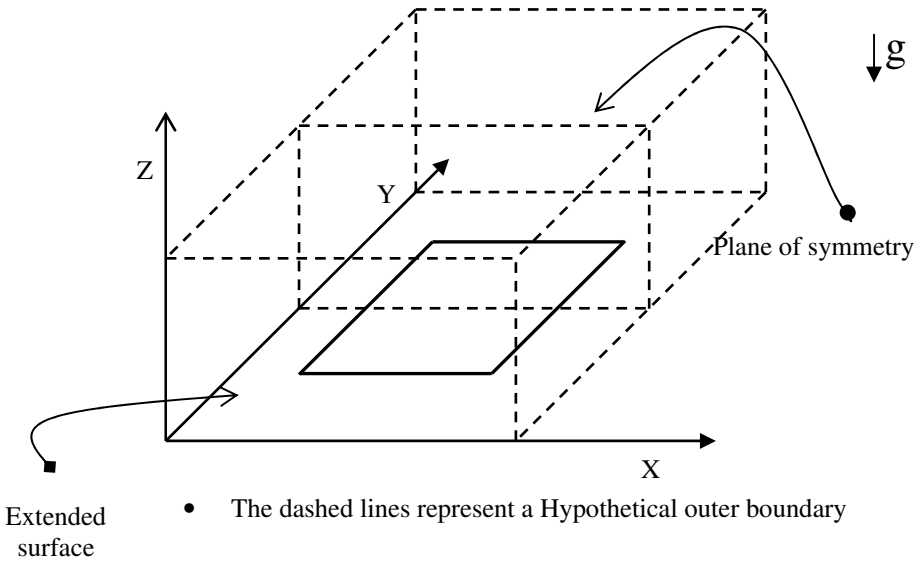

Fig (1): Dimensionless Coordinates for a Horizontal Square Plate and 3-D computational domain

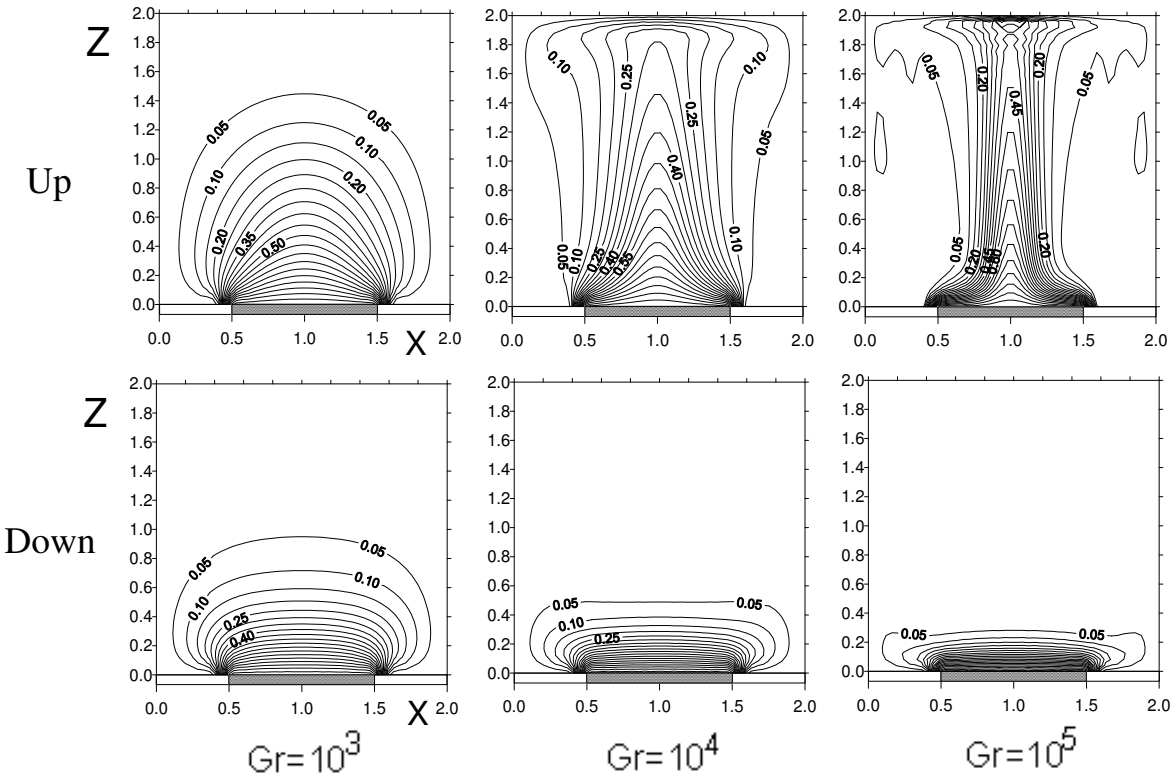

Fig(2):Steady State Temperature At Section Y=1/2 In X-Z Plane

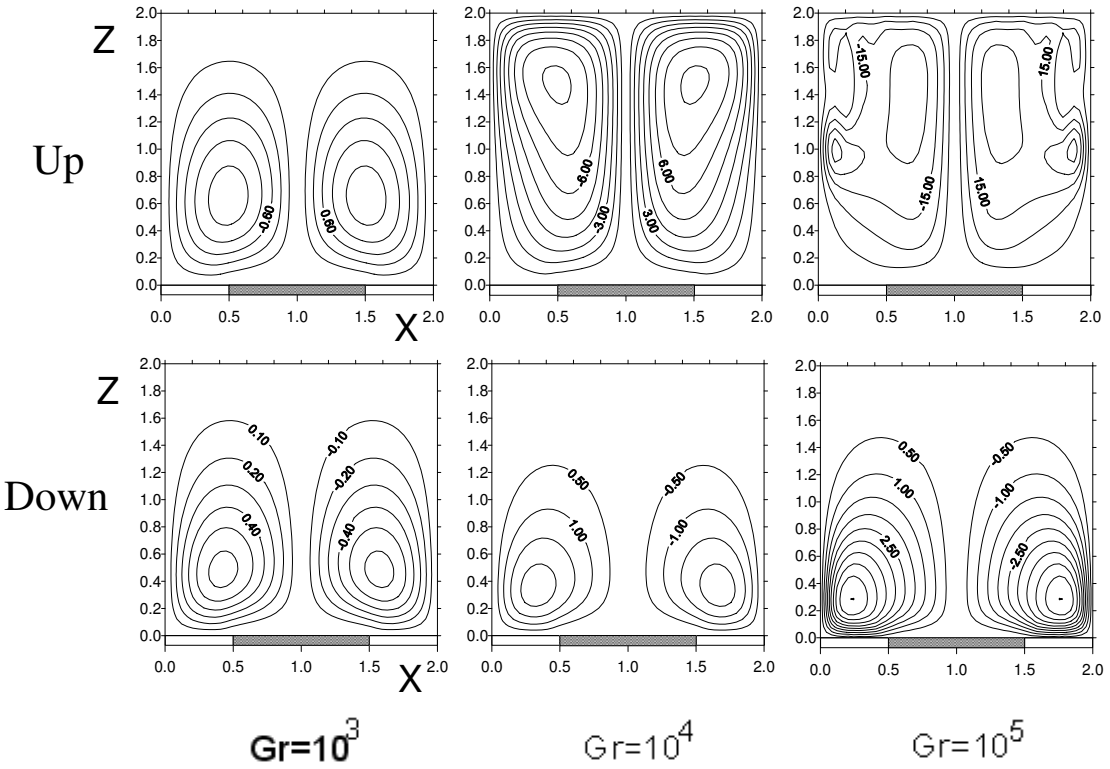

Fig(3): Steady State of Ψ_2 At Section Y=1/2 In X-Z Plane

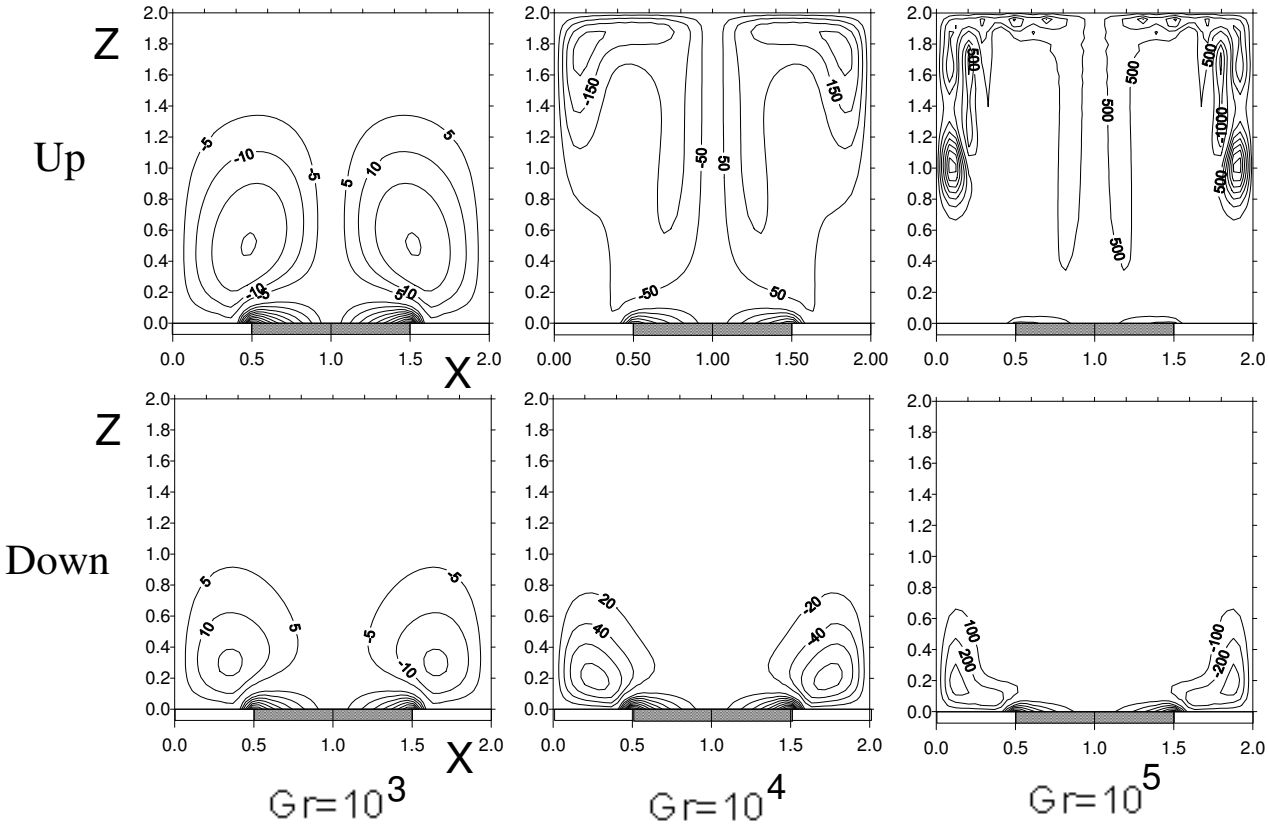

Fig(4):Steady State of Ω_2 At Section Y=1/2 In X-Z Plane

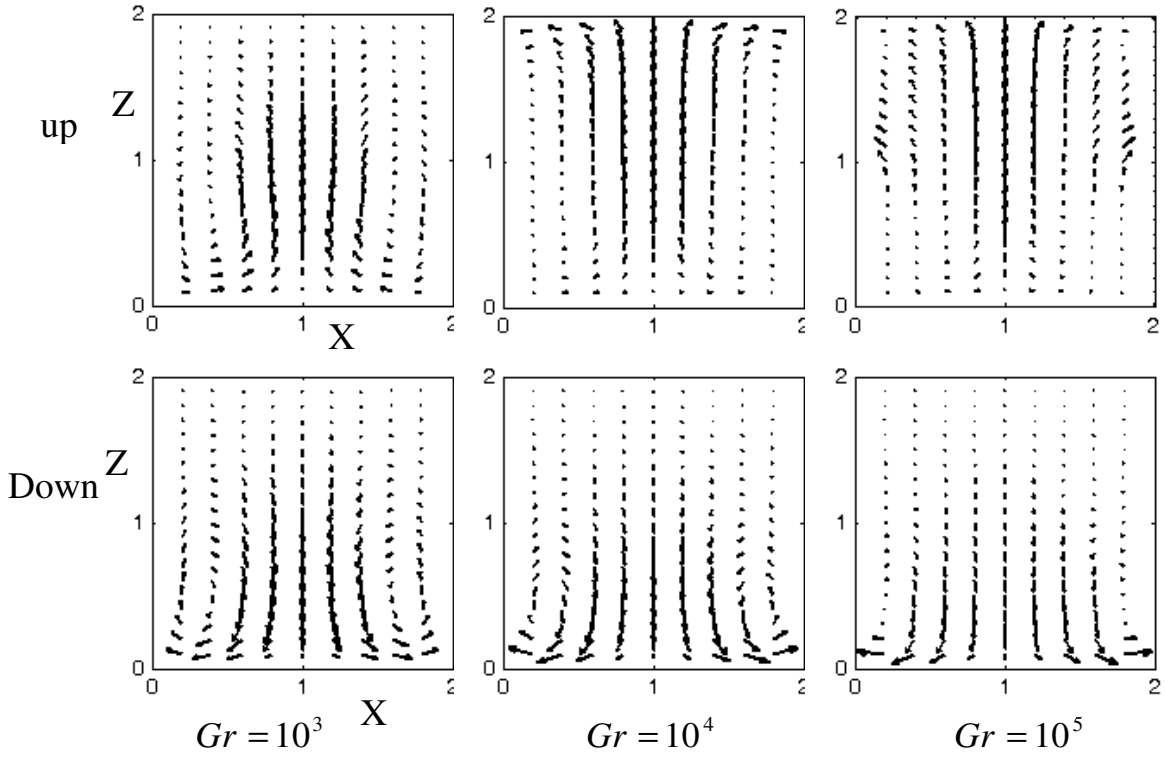

Fig(5):Steady State of Velocity Vector at Section Y=1/2 In X-Z Plane

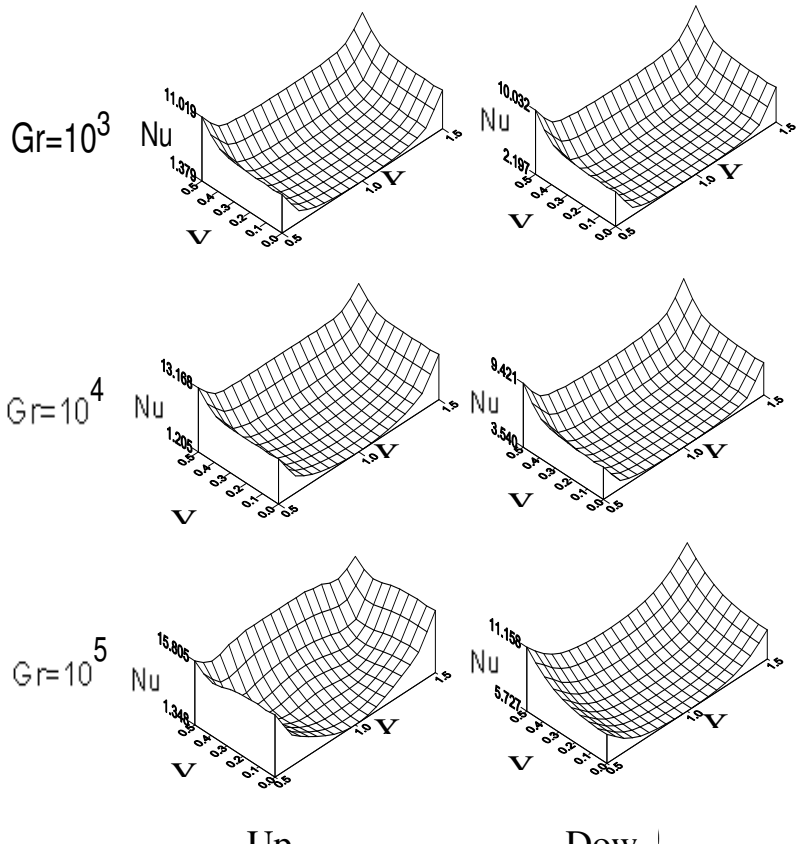

Fig.6 :Steady State of Local Nusselt Number Distribution over plate surface

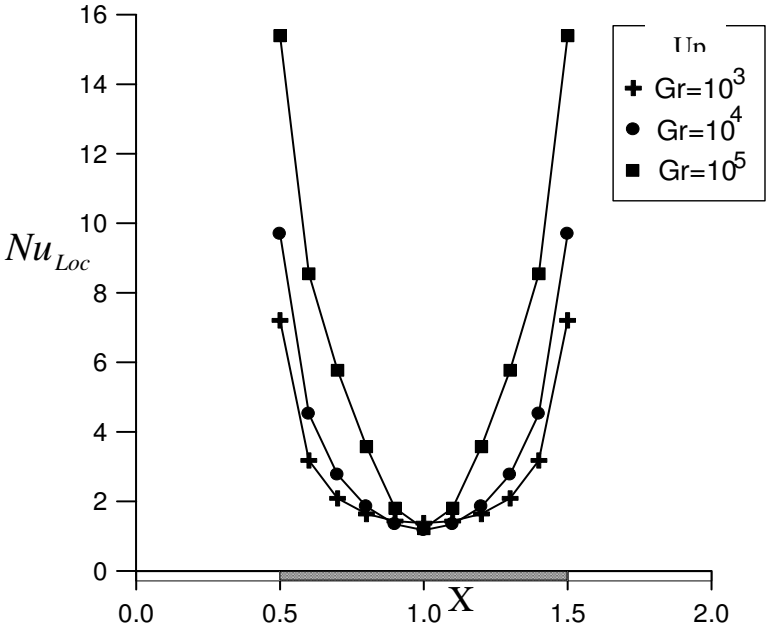

Fig.7 :Steady State of Local Nusselt Number Distribution at Y=1/2 For Up Ward Facing

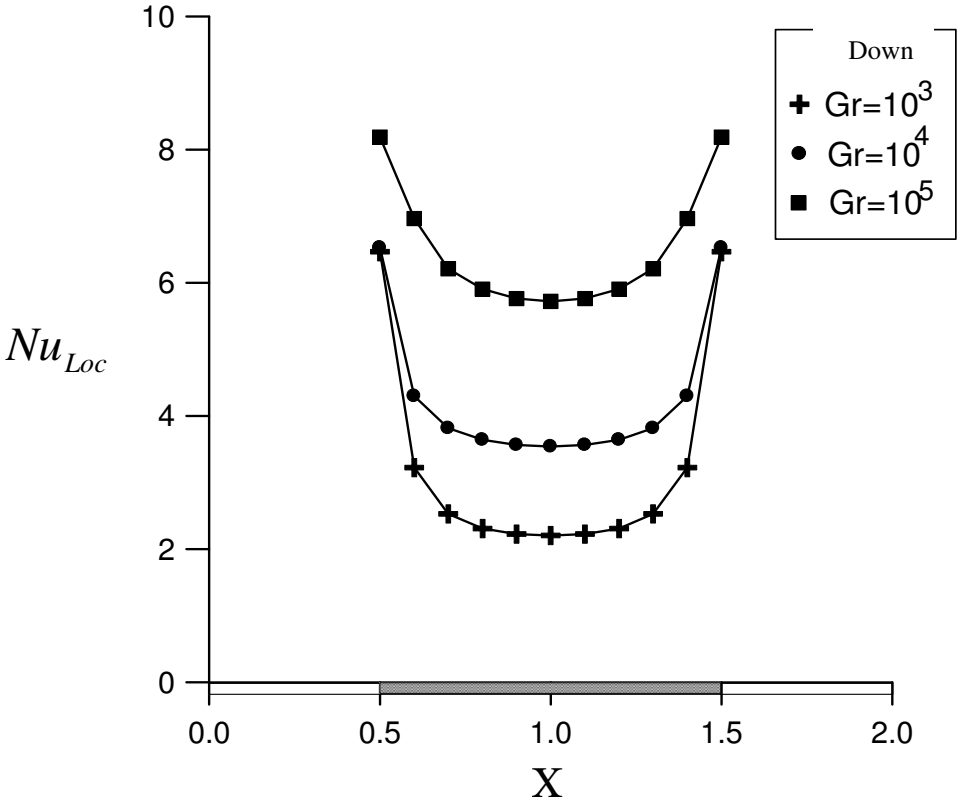

Fig.8 :Steady State of Local Nusselt Number Distribution at Y=1/2 For Down Ward Facing

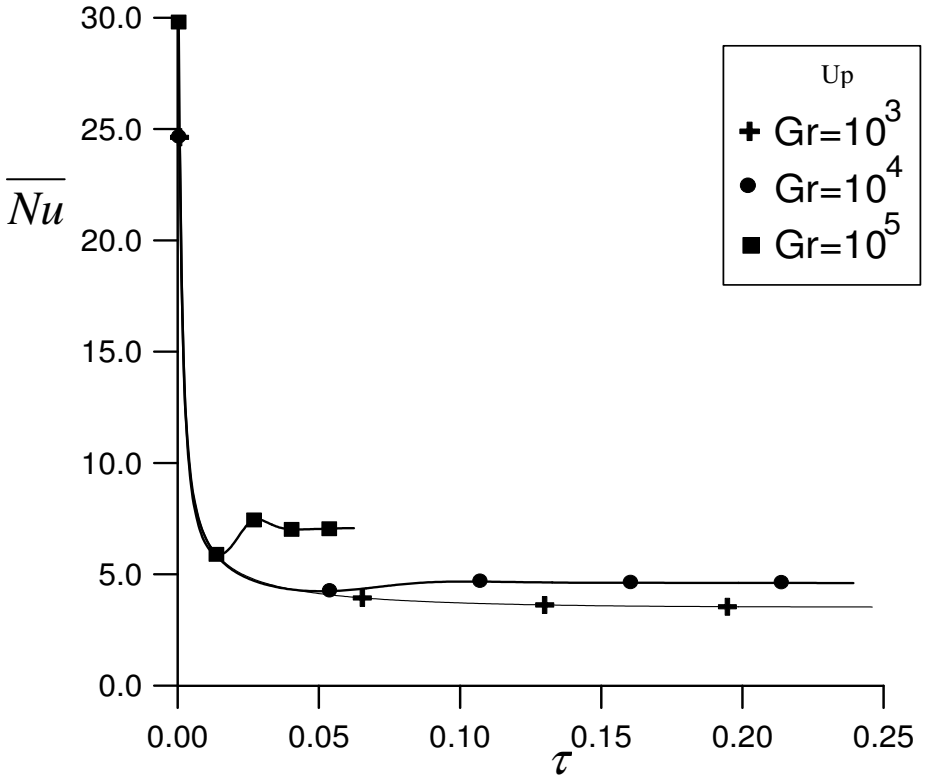

Fig.9 :Transient of Average Nusselt Number for Up Ward Facing

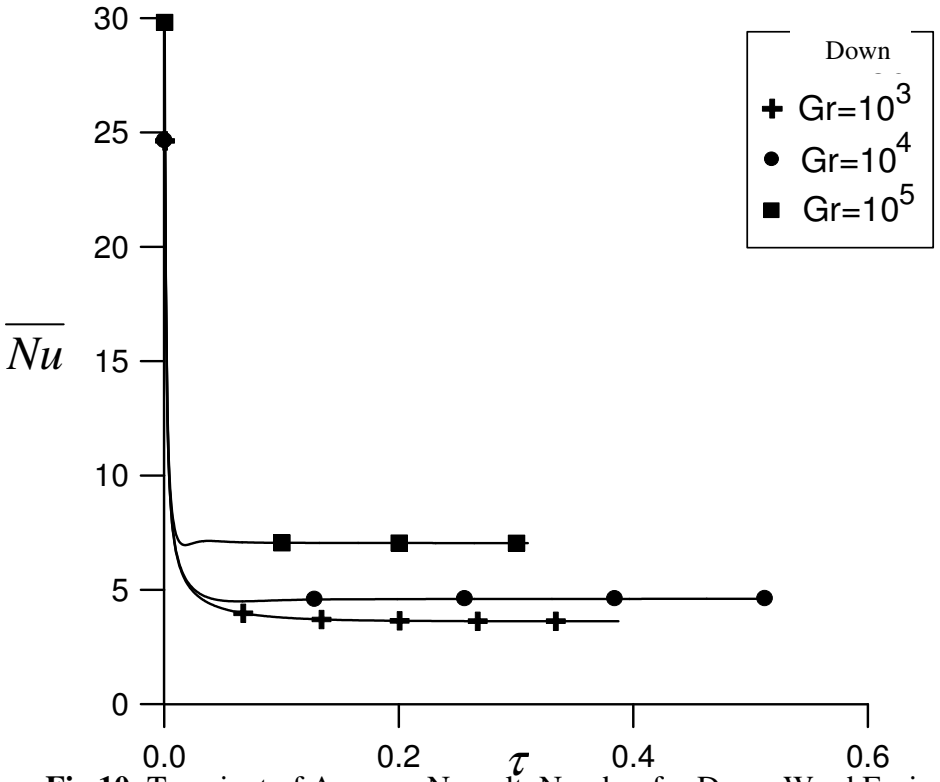

Fig.10 :Transient of Average Nusselt Number for Down Ward Facing

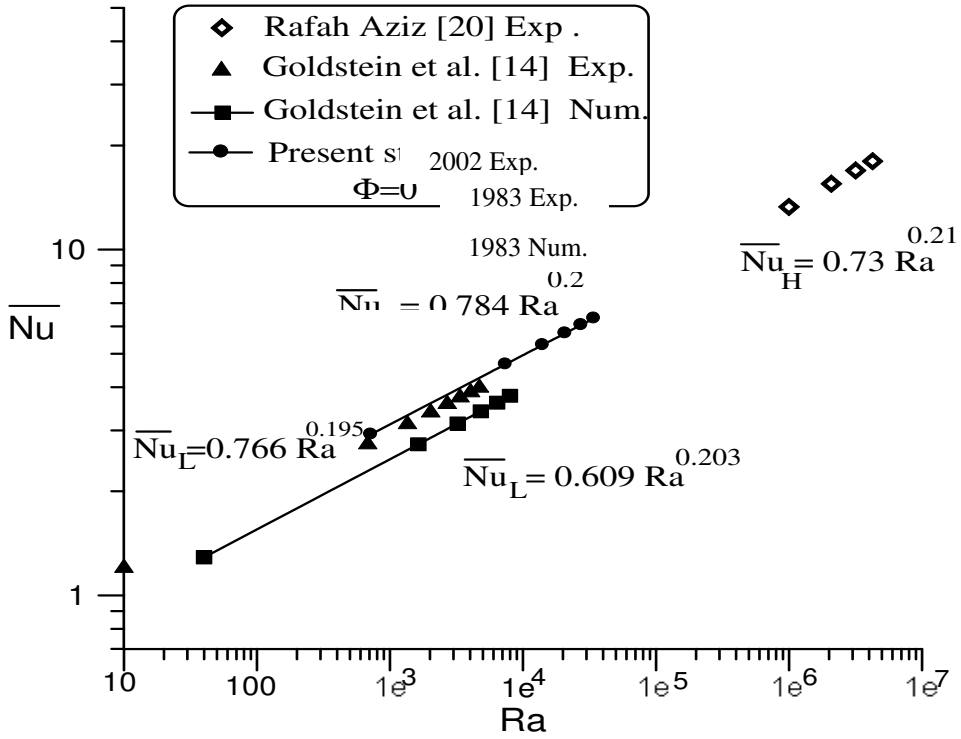

Fig.11 : Comparison with the Available Data for Horizontal Plate Facing upward

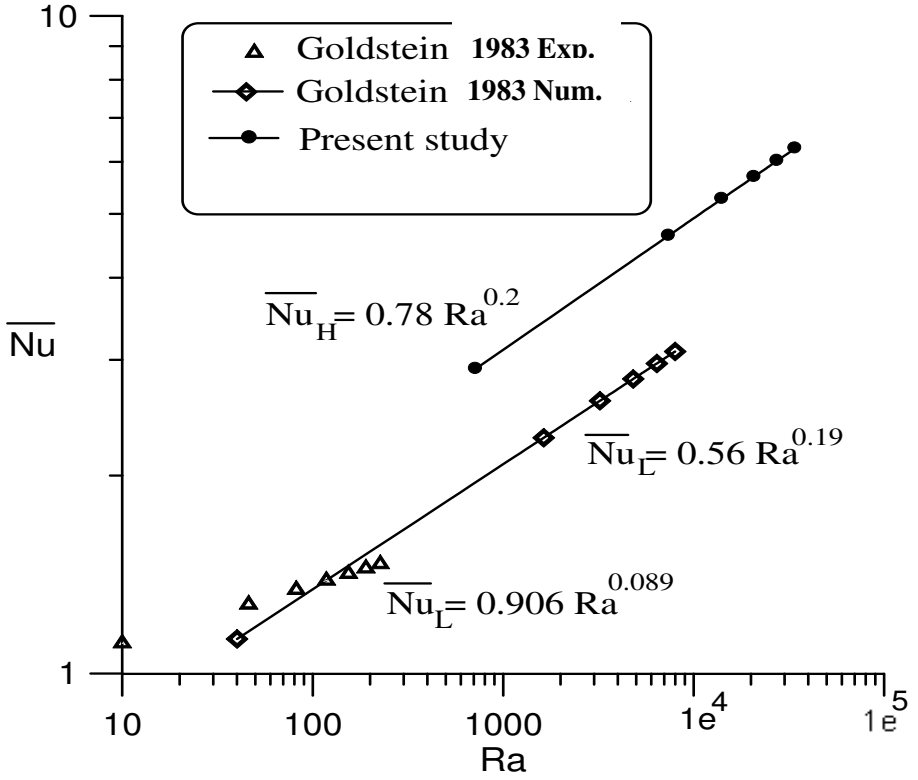

Fig.12 : Comparison with the Available Data for Horizontal Plate Facing Downward